

Probing compressed mass spectra in electroweak supersymmetry with Recursive Jigsaw Reconstruction

M. Santoni^{a,b}

^a*University of Adelaide, Department of Physics, Adelaide, SA 5005, Australia*

^b*ARC Centre of Excellence for Particle Physics at the Tera-scale, University of Adelaide*

E-mail: marco.santoni@adelaide.edu.au

ABSTRACT: The lack of evidence for the production of colored supersymmetric particles at the LHC has increased interest in searches for superpartners of the electroweak SM gauge bosons, namely the neutralinos and charginos. These are challenging due to the weak nature of the production process, and the existing discovery reach has significant gaps in due to the difficulty of separating the supersymmetric signal from SM diboson events that produce similar final states and kinematics. We apply the Recursive Jigsaw Reconstruction technique to study final states enriched in charged leptons and missing transverse momentum, focusing on compressed topologies with direct production of charginos and neutralinos decaying to the lightest neutral supersymmetric particle through the emission of W and Z bosons. After presenting prototype analysis designs for future LHC runs, we demonstrate that its detectors have the potential to probe a significant amount of unexplored parameter space for chargino-neutralino associated production within the next few years, and show that the very challenging successful search for chargino pair production with compressed spectra might be possible by the end of the LHC lifetime.

Contents

1	Introduction	1
2	The simplified compressed decay tree	2
3	Compressed electroweakino production in leptonic channels	4
3.1	Chargino-neutralino associated production in final states with three leptons and missing transverse momentum	5
3.2	Chargino pair production in final states with two leptons and missing transverse momentum	10
4	Conclusions	17

1 Introduction

The Standard Model (SM) of particle physics provides a successful explanation for a multitude of phenomena, but is considered an effective field theory of an underlying model valid at higher energies. Supersymmetry (SUSY) [1–8] refers to an invariance under generalized space-time transformations linking bosons and fermions. For each Standard Model particle it is postulated that there exists a partner with spin differing by one-half unit and other quantum numbers unchanged. Evidence of supersymmetric particles with mass at the electroweak-TeV scale are a sought-after experimental outcome, providing an explanation for the stabilization of the Higgs mass and potential gauge coupling unification.

R-parity conserving SUSY phenomenology demands an even number of superparticles in each interaction. Consequently, at a collider experiment, super-partners would be pair-produced, providing in the final state two stable lightest supersymmetric particles (LSPs). As the LSP interacts only weakly, escaping the detector, it assumes the characteristics compatible with a dark matter candidate. At the Large Hadron Collider (LHC) the missing transverse momentum ($\vec{\cancel{E}}_T$) can infer the presence of unmeasured weakly interacting particles. As the momentum in the transverse plane is conserved any missing momentum can be assumed to arise from missing particles including the LSPs.

Reconstruction techniques suffer from the lack of information related to the multiplicity and the masses of the particles not interacting with the detector. The difficulty is exacerbated in situations where the momenta of the weakly interacting particles is low. This is the case for supersymmetric spectra in which the difference in mass between the pair-produced parent superparticles \tilde{P} and the LSPs is low. Scenarios with a small mass-splitting are referred to herein as *compressed* [9].

In the compressed regime, visible and invisible decay products have low transverse momenta, as the center-of-mass system of the parent superparticles does. In this scenario,

the efficacy of typical variables [10] exploited to distinguish signal from background, based on large object transverse momenta and missing transverse energy, is limited.

One can gain indirect sensitivity by observing the reaction of the LSP pair to a probing force. The initial state radiation (ISR) from the interacting partons is the natural probe provided in the laboratory of a hadron collider. The ISR can boost the sparticles produced in these reactions and in turn endow their decay products with its momentum.

The Recursive Jigsaw Reconstruction technique has been used by the ATLAS collaboration to probe supersymmetric scenarios in cases involving the production of colored superpartners of SM particles [11]. In the compressed regime, a general basis of kinematic observables designed for the analysis of events with initial state radiation can be used independently from the topology investigated. In this paper we focus on applications of this technique to final states in the electroweak SUSY sector.

Electroweakinos are a linear combination of the fermionic partner of the gauge bosons and the two Higgs bosons. Neutral higgsinos and gauginos mix to form four eigenstates of mass called neutralinos ($\tilde{\chi}_i^0$ with $i = 1, 2, 3$ or 4) while charged winos and higgsinos form two eigenstates of mass referred to charginos ($\tilde{\chi}_i^\pm$ with $i = 1$ or 2). Herein one assumes the lightest neutralino is the LSP and focuses on cases with small mass difference between it and the $\tilde{\chi}_1^\pm$ and/or $\tilde{\chi}_2^0$. Compressed scenarios involving electroweakinos are common in supersymmetric theory. For example, in naturalness-inspired models [12] the higgsino components are light, hence small mass splittings are expected for the lower eigenstates of mass of higgsino-like charginos and neutralinos. At the same time the masses of the wino components, appearing in the one-loop corrections to the Higgs mass, are expected to be limited.

Qualitatively, the smaller the mass difference between the parent superparticle and the LSP, $\Delta M = M_{\tilde{P}} - M_{\tilde{\chi}_1^0}$, the less opportunity there is to accommodate an additional intermediate superparticle. In this study, final states arising from intermediate sleptons are not considered. We focus on simplified topologies where $\tilde{\chi}_1^\pm \rightarrow W^\pm \tilde{\chi}_1^0$ and $\tilde{\chi}_2^0 \rightarrow Z \tilde{\chi}_1^0$. For a mass splitting below the W -boson mass, two-body decays are kinematically suppressed and we generate three-body decays involving off-shell bosons and assume other mediators do not contribute.

2 The simplified compressed decay tree

Recursive Jigsaw Reconstruction (RJR) [13] is a HEP technique based on the imposition of a decay tree mimicking the signal topology investigated. A series of algorithms, referred to as jigsaw rules, are applied to solve final state ambiguities due to unknown kinematic degrees of freedom when weakly interacting particles are present and combinatoric challenges due to the presence of indistinguishable visible particles from a detector prospective. The result is an estimate of the relevant reference frames and hence, a complete basis of kinematic observables sensitive to the masses and decay angles of the resonances appearing in the chosen tree, which can be used to distinguish signatures of new physics from the SM background.

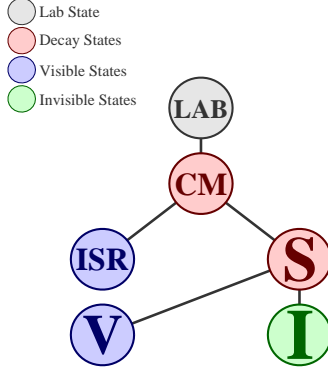


Figure 1: The simplified decay tree diagram for the analyses of compressed signal topologies.

In RJR involving compressed scenarios the simplified decay tree shown in Figure 1 is used for analyzing topologies with initial state radiation. A transverse view of the event is considered, namely all the z -momenta of the visible objects are set to zero.

We follow the procedure outlined in [14]. The estimate for the center-of-mass system of the whole reaction SUSY + ISR is labeled by CM, ISR is the system assigned to the radiation from the initial state, S is the signal or sparticle system decaying in visible and invisible products and hence to the V and I systems. In each event, the missing transverse momentum is assigned to the I-system, while a jigsaw rule specifies the reconstructed objects hypothesized to come from the decay of sparticles and assigned to the V-system with respect to those associated with ISR.

Topology independent observables include:

- $R_{\text{ISR}} \equiv \frac{|\vec{p}_{\text{I},T}^{\text{CM}} \cdot \vec{p}_{\text{ISR},T}^{\text{CM}}|}{p_{\text{ISR},T}^{\text{CM}}}$: variable sensitive to the mass ratio between LSP and parent superparticle.
- $p_{\text{ISR},T}^{\text{CM}}$: magnitude of the vector-sum of the jets transverse momenta of the ISR-system evaluated in the CM frame.
- $\Delta\phi_{\text{ISR},\text{I}}$: opening angle between the ISR-system and the I-system, evaluated in the CM frame.

In final states with two LSPs and no other weakly interacting particles the observable R_{ISR} can be written in the laboratory frame as

$$R_{\text{ISR}} \sim \frac{|\vec{E}_T \cdot \hat{p}_T^{\text{ISR}}|}{p_T^{\text{ISR}}} \sim \frac{M_{\tilde{\chi}_1^0}}{M_{\tilde{P}}} + \mathcal{O}\left(\frac{p_{\tilde{\chi}_1^0}^{\tilde{P}}}{2M_{\tilde{P}}}\right) \left(\frac{\sqrt{(p_T^{\text{ISR}})^2 + m_{\tilde{P}\tilde{P}}^2}}{p_T^{\text{ISR}}}\right) \sin \Omega. \quad (2.1)$$

This approximation is valid for the extreme compressed scenarios, hence in the limit of a low-momentum of the LSP in the parent superparticle rest frame $p_{\tilde{\chi}_1^0}^{\tilde{P}}$ with respect to the parent superparticle mass $M_{\tilde{P}}$, while $m_{\tilde{P}\tilde{P}}$ is the true mass of the S-system and $\sin \Omega$ is a quantity which is zero on average. The observable scales with the mass ratio $M_{\tilde{\chi}_1^0}/M_{\tilde{P}}$

and width of order $p_{\tilde{\chi}_1^0}^{\tilde{P}}/2M_{\tilde{P}}$ in the limit $p_T^{ISR} \gg m_{\tilde{P}\tilde{P}}$. When visible decay objects are not reconstructed in the V-system or additional neutrinos in the final state contribute to the missing transverse momentum, R_{ISR} is expected to assume values between the mass ratio and one with smaller resolution.

3 Compressed electroweakino production in leptonic channels

Simulated Monte Carlo (MC) samples of Standard Model backgrounds and SUSY signals are used to study distributions of the performance of the RJR observables. The SM background processes expected to be the largest contributions have been generated elsewhere [15]. These samples are proton proton collisions at $\sqrt{s} = 14$ TeV generated with MadGraph 5 [16]. The parton shower and hadronization is performed with Pythia 6 [17] followed by a detailed detector simulation with Delphes 3 [18] in which a parameterization for the performance of the existing ATLAS [21] and CMS [22] experiments is implemented. Jets are reconstructed by the anti- k_T clustering algorithm [19] with $R = 0.5$ and $p_T^{\text{min}} = 20$ GeV, implemented with the FastJet [20] package. The simulation procedure involves generation of events at leading order in bins of the scalar sum of the generator level particles transverse momenta, with jet-parton matching and corrections for next-to-leading order (NLO) contributions [23].

The same procedure and parametrization are used to generate the signal samples. The topologies considered are associated chargino-neutralino production and chargino pair production assuming degenerate masses $M_{\tilde{\chi}_1^\pm} = M_{\tilde{\chi}_2^0}$, $M_{\tilde{\chi}_1^+} = M_{\tilde{\chi}_1^-}$ in the range $100 \text{ GeV} \leq M_{\tilde{P}} \leq 500 \text{ GeV}$ in the compressed regime: the mass splittings considered are in the range $15 \text{ GeV} \leq \Delta M \leq 75 \text{ GeV}$.

The cross sections for pure wino chargino pair production and chargino-neutralino associated production at $\sqrt{s} = 13$ TeV at NLL can be found elsewhere [24, 25] with relative uncertainties in the range $4.5\% \lesssim \Delta\sigma \lesssim 9\%$ for the masses investigated. We estimate the NLL cross sections at $\sqrt{s} = 14$ TeV, evaluating the NLO cross sections for the wino-like electroweakino pair production at 13 and 14 TeV with Madgraph and assuming the same NLL/NLO k -factors for the corrections. The resulting NLL cross sections are shown in Figure 2a and used as inputs for the analysis of the simplified supersymmetric topologies. This procedure provides small corrections ($\lesssim 5\%$) from the k -factors and is a check for the matched Madgraph cross sections and their potential dependences on the cutoff scales chosen.

The focus of this work is on the leptonic decay channels of off-shell W and Z bosons, as depicted in the Feynman diagrams in Figure 2b and Figure 2c. Leptonic final states from charmonium and bottomonium are expected to be negligible in the phase space probed.

Focusing on electrons and muons as visible decay products provides several advantages. Firstly, the signal-to-background ratio increases progressively with lepton multiplicity in the final state. Secondly, the channels result in clean final states with high efficiencies for the lepton reconstruction: in this study one assumes the minimum value for reconstructed lepton p_T of 10 GeV. Recent work by the CMS collaboration has demonstrated improvements in the efficiency of identification of *soft* isolated electrons and muons (down to $\sim 3\text{-}4$ GeV) [26].

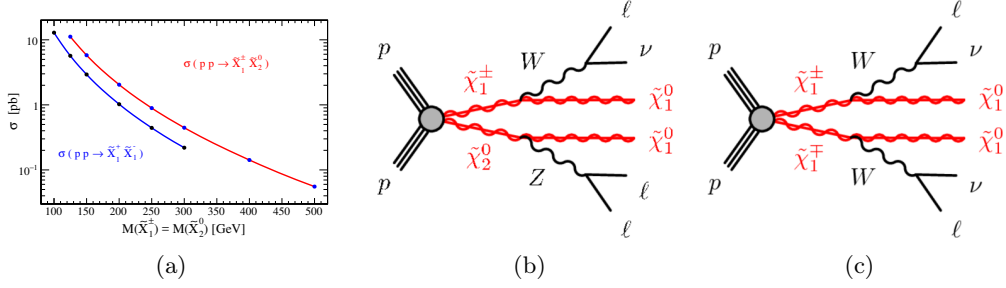


Figure 2: Estimated NLL cross sections for pure wino chargino pair production (blue curve) and chargino-neutralino associated production (red curve) at $\sqrt{s} = 14$ TeV (a). Feynman diagrams for electroweakino productions in final states with missing transverse momentum and three charged leptons (b) or two charged leptons (c).

Moreover, for our purposes all leptons are identifiable as reconstructed objects produced via sparticle decays and hence they are assigned to the V-system, while all the jets can be assigned to the ISR-system with no ambiguity. This allows us to avoid focusing solely on the high ISR regime in order to exploit the compressed RJR strategy. A minimal value of the transverse momentum of the ISR-system, in concert with \cancel{E}_T , can elicit an increase in the transverse momenta of the decay products of the SUSY system. In this way we can leverage the RJR technique for compressed scenarios without requiring a restrictive event selection based on a huge value of the ISR transverse momentum.

3.1 Chargino-neutralino associated production in final states with three leptons and missing transverse momentum

The signal samples are the simplified topologies as in Figure 2b generated within the mass ranges $125 \text{ GeV} \leq (M_{\tilde{\chi}_1^\pm} = M_{\tilde{\chi}_2^0}) \leq 500 \text{ GeV}$, with five mass splittings $\Delta M = M_{\tilde{P}} - M_{\tilde{\chi}_1^0} = 15, 25, 35, 50$ and 75 GeV . Event-by-event a basis of RJR variables is extracted and analyzed to probe compressed spectra for a projection of $\int \mathcal{L} dt = 300 \text{ fb}^{-1}$. To the previous variables, additional transverse observables for this study include:

- M_T^V : transverse mass of the V-system.
- M_{l+l-} : transverse mass of the two same flavor opposite sign leptons in final state where the third lepton has different flavor (M_{T, e^+e^-} when the third lepton is a muon and $M_{T, \mu^+\mu^-}$ when the third lepton is an electron).
- $\Delta\phi_{\text{CM}, \text{I}}$: opening angle between the CM system and the I-system.

Three leptons (electrons and muons) are required in the final state with $p_T > 10 \text{ GeV}$, while at least one jet with $p_T > 20 \text{ GeV}$ is associated to the ISR-system. A minimal value for the transverse missing momentum is the last preselection requirement: $\cancel{E}_T > 50 \text{ GeV}$.

Figure 3 shows the distributions of R_{ISR} and $p_{\text{ISR}, T}^{\text{CM}}$ after preselection criteria are imposed. All of the relevant Standard Model backgrounds are stacked together and categorized into five groups. The main contributions are WZ boson associated production and

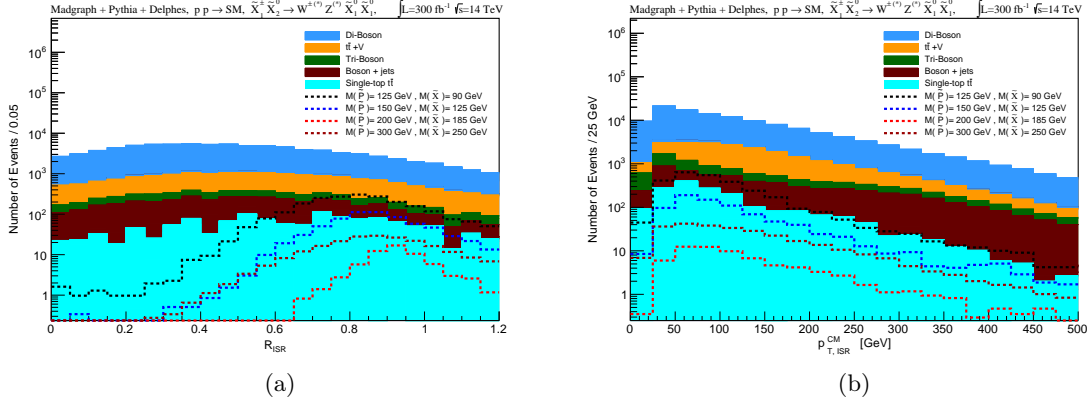


Figure 3: Distributions of $R_{\text{ISR}} = \frac{|p_{I,T}^{\text{CM}} \cdot p_{\text{ISR},T}^{\text{CM}}|}{p_{\text{ISR},T}^{\text{CM}}}$ (a) and $p_{\text{ISR},T}^{\text{CM}}$ (b) for events that have satisfied the preselection criteria. All the contributions are scaled with an integrated luminosity of 300 fb^{-1} at $\sqrt{s}=14 \text{ TeV}$.

$t\bar{t}$ processes with an additional vector boson. The overlaid dashed curves refer to four chargino-neutralino production samples with different masses and mass splittings.

The observable R_{ISR} provides a remarkable signal-to-background discrimination in the absence of more stringent selection criteria as shown in Figure 3a. The assignment of the different objects in the compressed tree is performed with no ambiguity, and it is not necessary to focus on the high ISR regime in order to improve the observable resolution for the signal samples. Notice that R_{ISR} can assume larger values than unity when some objects are forced in the V -system. The observable is expected to be peaked for values beyond $M_{\tilde{\chi}}/M_{\tilde{P}}$ due to the additional contribution to \cancel{E}_T coming from one or more neutrinos. Values larger than the mass ratio will be considered for the definition of the R_{ISR} requirements together with $R_{\text{ISR}} < 1$.

Figure 3b shows the distribution of $p_{\text{ISR},T}^{\text{CM}}$. The scales for the signal and background samples are similar and the variable has limited impact. In the absence of other requirements the slope for the signal is paradoxically more severe arising from the background events with non-radiative jets, forced into the ISR-system. A minimal requirement on $p_{\text{ISR},T}^{\text{CM}}$ is essential to exploit the RJR technique with multi-lepton final states. The requirement applied to this variable, being the only large scale observable in this study together with \cancel{E}_T , will be moderately tighter for large mass splittings, when the criterion on R_{ISR} is relaxed.

It is interesting to note that the number of events passing the preselection criteria is smaller for the signal sample with $M_{\tilde{\chi}_1^\pm} = M_{\tilde{\chi}_2^0} = 200 \text{ GeV}$ and $\Delta M = 15 \text{ GeV}$ compared to the sample with $M_{\tilde{\chi}_1^\pm} = M_{\tilde{\chi}_2^0} = 300 \text{ GeV}$ and $\Delta M = 50 \text{ GeV}$. There has been a conservative minimal choice of transverse momentum for electrons and muons of 10 GeV and when the mass splitting approaches a much more compressed regime, the kinematics are such that one of the three leptons is less likely to satisfy this transverse momentum constraint. In order to probe the extreme compressed regime ($\Delta M < 15 \text{ GeV}$) a parametrization of the efficiency

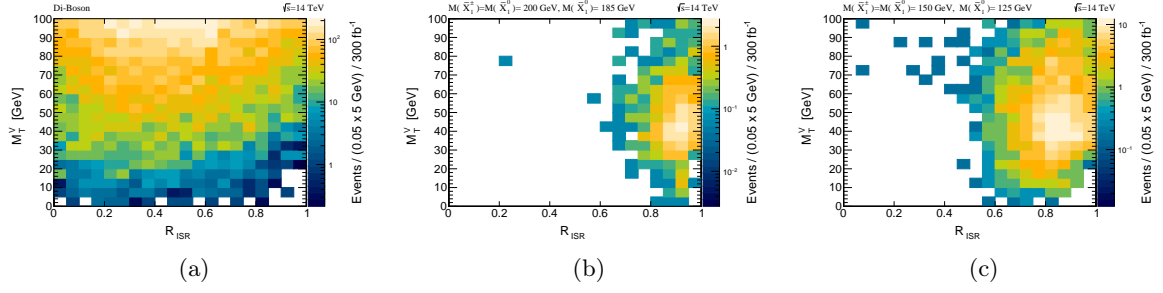


Figure 4: Distribution of the M_T^V as a function of R_{ISR} for the di-boson background (a) and the signal samples $M_{\tilde{\chi}_1^\pm} = M_{\tilde{\chi}_2^0} = 200$ GeV, $M_{\tilde{\chi}_1^0} = 185$ GeV (b) and $M_{\tilde{\chi}_1^\pm} = M_{\tilde{\chi}_2^0} = 150$ GeV, $M_{\tilde{\chi}_1^0} = 125$ GeV (c). One demands preselection criteria, $N_{b\text{-jet}}^{\text{ISR}} = 0$, $p_{\text{ISR},T}^{\text{CM}} > 50$ GeV and $M_T^V < 100$ GeV.

in the reconstruction of soft electron and muons with transverse momenta ($p_T \lesssim 10$ GeV) must be implemented. This is considered beyond the scope of this paper due to the difficulty of getting these details correct outside of an experimental collaboration.

Figure 4 shows the two dimensional distributions of M_T^V as a function of R_{ISR} for the main Standard Model background and two representative signal samples for events passing the preselection criteria, and after applying a veto for jets tagged as being initiated by a b -quark ($N_{b\text{-jet}}^{\text{ISR}} = 0$). The final state signal events populate low values of M_T^V with a complementarity with high values of R_{ISR} . Vice versa, for the di-boson background, simultaneous low values of M_T^V and R_{ISR} close to one are disfavored as shown in Figure 4a.

Using the two RJR observables in concert provides an increasingly powerful discrimination the smaller the absolute and relative mass splitting of the signal sample. In the low M_T^V regime ($M_T^V < 100$ GeV), and for values of the ratio close to unity ($R_{\text{ISR}} > 0.6$) additional handles to decrease the SM background yields are provided by the compressed-transverse RJR angles and M_{l+l-} . Figure 5 shows the distribution of $\Delta\phi_{\text{ISR},I}$ (a), $\Delta\phi_{\text{CM},I}$ (b) and M_{l+l-} for final state events with only two of the three leptons with same flavor (c). For the signal events, the transverse mass of the two leptons has a clean end-point at the expected ΔM .

Selection criteria applied on the compressed RJR observables, as shown in Table 1, can be used to define signal regions for probing chargino-neutralino associated pair production in final states with three leptons and missing transverse momentum. One or more additional jets is assumed to be radiated from the initial state and a minimal requirement on $p_{\text{ISR},T}^{\text{CM}}$ (and \cancel{E}_T) allows us to focus on the final states of interest and probe the compressed spectra. The signal regions target five particular mass splittings. A special treatment is assumed for the selection criteria applied to R_{ISR} , since this observable is related to the mass ratio $M_{\tilde{\chi}}/M_{\tilde{P}}$ rather than the absolute value of the mass splitting. Tighter selection criteria are used for the only large scale variables ($p_{\text{ISR},T}^{\text{CM}}$ and \cancel{E}_T), the jet multiplicity and $\Delta\phi_{\text{CM},I}$ when for larger mass differences ($\Delta M = 50, 75$ GeV) the R_{ISR} requirement is relaxed. Low

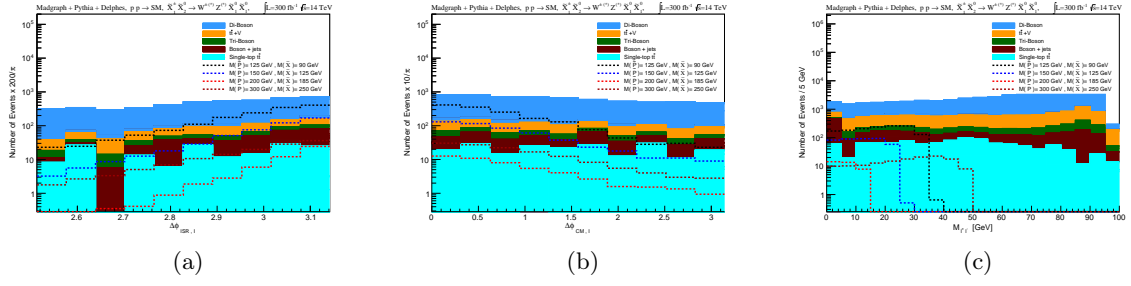


Figure 5: Distributions of $\Delta\phi_{\text{ISR},I}$ (a), $\Delta\phi_{\text{CM},I}$ (b) and M_{l+l-} (c) for the events satisfying the preselection criteria, $N_{b\text{-jet}}^{\text{ISR}} = 0$, $p_{\text{ISR},T}^{\text{CM}} > 50$ GeV, $M_T^Y < 100$ GeV and $R_{\text{ISR}} > 0.6$.

Variable	Mass Splitting [GeV]				
	$\Delta M = 15$	$\Delta M = 25$	$\Delta M = 35$	$\Delta M = 50$	$\Delta M = 75$
Object multiplicity selection criteria	3 Leptons (e and μ) with $p_T^{\text{lep}} > 10$ GeV, At least one jet, $p_T^{\text{jet}} > 20$ GeV, $N_{b\text{-jet}}^{\text{ISR}} = 0$				
$p_{\text{ISR},T}^{\text{CM}} (\cancel{E}_T) > [\text{GeV}]$	50			70	120
$N_{\text{jet}}^{\text{ISR}} <$	3	4		3	
$M_T^Y <$, for 3 SFL [GeV]	40	50	65	75	90
$M_{l+l-} <$, for 2 SFL [GeV] ($M_T^Y < 100$ GeV)	15	25	35	50	75
$\Delta\phi_{\text{CM},I} <$	1			0.7	0.5
$\Delta\phi_{\text{ISR},I} >$	3				
$R_{\text{ISR}} >$	0.85, 0.9	0.8, 0.85 0.9	0.8, 0.85	0.7, 0.8 0.85	0.65, 0.7 0.75

Table 1: A loosely optimized set of selection criteria for signal regions in the analysis of chargino neutralino production in final states with three leptons and missing energy.

values are required for M_T^Y , progressively more stringent to the decrease of ΔM , while for M_{l+l-} , one requires a maximum defined exactly by the mass splitting itself. In final states with three electrons or three muons only the M_T^Y requirement is applied, while for events with two same and one different flavor leptons the selection on M_{l+l-} is required together with $M_T^Y < 100$ GeV. The selection criteria applied to the observable R_{ISR} are progressively more stringent the closer the mass ratio to unity and the values are separated by 0.05, which provides a moderate optimization. Figure 6 shows the distributions of $\Delta\phi_{\text{CM},I}$ and M_T^Y applying respectively the N-1 requirements in column 2 and 3 of Table 1.

The signal regions expressed by the selection criteria of the RJR observables defined in Table 1 are applied to calculate projected sensitivities for compressed spectra signal samples. Figures 7 shows the value of Z_{Bi} calculated assuming the metric [27] at $\sqrt{s}=14$ TeV for an integrated luminosity of 300 fb^{-1} . A systematic uncertainty of 20% is assumed for the

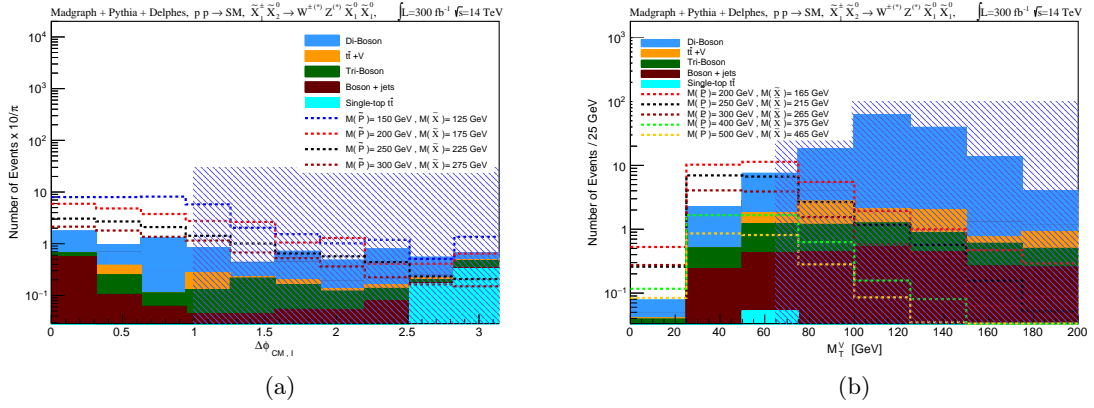


Figure 6: The distributions of the observables $\Delta\phi_{CM,I}$ and M_T^Y for signal and Standard Model background events passing the N-1 selection criteria in one of the signal regions of Table 1 with $R_{ISR} > 0.85$.

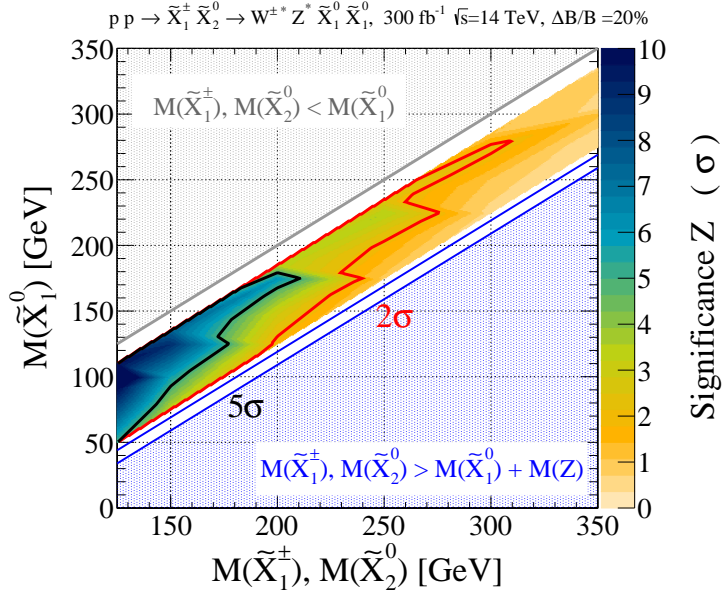


Figure 7: Projected exclusion and discovery reach for chargino-neutralino associated production in the compressed region ($15 \text{ GeV} \leq \Delta M \leq 75 \text{ GeV}$) at $\sqrt{s} = 14 \text{ TeV}$ for an integrated luminosity of 300 fb^{-1} .

whole signal grid with the main contribution to the background arising from associated WZ production.

The highest impact of the compressed RJR observables are for the samples of mass splittings in the range 20-40 GeV, a challenging phase space for SUSY searches [28]. The signal yields in the extreme compressed scenarios can benefit from an improvement in the efficiencies of the detector in the reconstruction of low-momentum leptons, which is outside the scope of this work. On the other hand, the significances decrease for mass differences

close to the W pole mass due the difficulty to discriminate background events derived from topologies with absolute and relative mass scales very close to the signal ones.

For an integrated luminosity of 300 fb^{-1} , degenerate charginos and neutralinos would be discovered for masses $M_{\tilde{\chi}_1^\pm} = M_{\tilde{\chi}_2^0} > 150 \text{ GeV}$ for a large portion of the samples investigated and excluded up to 300 GeV for the best scenarios.

The value $\Delta M = 15 \text{ GeV}$ must not be considered as a threshold: the minimum mass difference achievable with any technique is strongly related to the efficiencies for the detector to reconstruct low-momentum leptons. For extremely compressed scenarios, a similar analysis could be used to probe the same final state topologies with only two low-momentum leptons reconstructed. Although the background would differ in that case, one could require two same-sign leptons to suppress the SM yield. Overall, one can improve the impact of the RJR technique by adopting a strategy based not only on transverse observables, but exploiting a three-dimensional reconstruction as in the following study.

3.2 Chargino pair production in final states with two leptons and missing transverse momentum

We now move on to consider a different and still more complicated compressed electroweakino investigation. The signal samples are simulated proton-proton collisions at $\sqrt{s} = 14 \text{ TeV}$ producing a pair of charginos with opposite electric charge and with $\tilde{\chi}_1^\pm \rightarrow W^{*\pm}(\rightarrow l^\pm \nu) \tilde{\chi}_1^0$. The focus is on final states with two leptons as illustrated in the simplified topology in Figure 2c. The samples are generated within the mass ranges $100 \text{ GeV} \leq M_{\tilde{\chi}_1^\pm} \leq 300 \text{ GeV}$, with the five mass splittings $\Delta M = M_{\tilde{P}} - M_{\tilde{\chi}} = 15, 25, 35, 50$ and 75 GeV .

The lepton multiplicity of the final state determines the main contributions of the Standard Model processes. The di-leptonic channels of a pair of W bosons, constitute the main processes resulting in a final state with two opposite sign leptons and missing transverse momentum, in the absence of hadronic jets. Searches for chargino pair production in final state with two leptons are challenging for open mass spectra due to the W^+W^- irreducible background, while other contributions are often negligible. In the compressed regime the difficulty is exacerbated by the low momenta of invisible and visible objects and the subsequent kinematics. Moreover, requiring a transverse momentum for the ISR-system introduces an additional complication for the analysis in the compressed regime: Standard Model backgrounds other than WW will contribute quite significantly.

In order to improve the signal-to-background discrimination one enriches the simplified version of the compressed RJR tree in Figure 1, by specifying the substructure of the S-system. This is feasible for the two leptons final state case when one has no ambiguity as to the provenance of the reconstructed visible sparticle decay products. These decay products can then be assigned to the appropriate position in the tree.

The RJR decay tree is shown in Figure 8. Electrons and muons are associated to the l^+ and l^- systems, depending to the electric charge, while the jets are assigned to the ISR-system. The S-system frame is the approximation for the center-of-mass of the two charginos and each one decays to a lepton and an invisible system. Each invisible system collects the $\tilde{\chi}_1^0 + \nu$ contribution of the hemisphere a and b .

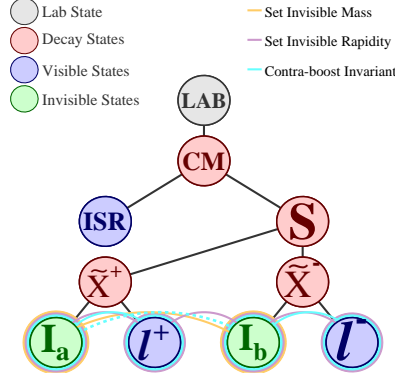


Figure 8: The decay tree for the analysis of compressed chargino pair production in events with ISR. The substructure of the S system is specified as follow: each chargino decays to a visible (lepton) and an invisible (neutrino + neutralino) object.

In this approach, a three dimensional view is considered and jigsaw rules are applied in order to reconstruct the topology and the relevant frames of reference. In the overall center-of-mass frame the ISR and S-systems are back-to-back. A Lorentz invariant jigsaw rule is assumed for the estimate of the mass of the invisible objects, while the rapidity is assigned to the chargino center-of-mass (equal to the rapidity of the visible objects in the S-system). Finally, a contra-boost invariant jigsaw rule partitions the remaining unknown degrees of freedom associated to I_a and I_b . More information can be found elsewhere [29, 30].

The useful transverse variables of the simplified tree can be computed along with additional experimental observables. Having in mind the simplified tree in Figure 1, one can reconstruct the I-system corresponding to the sum of the two invisible systems $I = I_a + I_b$ and V to the sum of the two lepton systems $V = l^+ + l^-$ and compute the transverse observables: R_{ISR} , $p_{\text{ISR},T}^{\text{CM}}$ and $\Delta\phi_{\text{ISR},I}$.

Three-dimensional scale-sensitive variables and additional angular observables include:

- M^V is the mass associated to the V-system: invariant mass of $(l^+ + l^-)$.
- $M^{\tilde{\chi}^\pm}$ is the mass associated with the chargino system.
- $\Delta\phi_{l^+,I}$ ($\Delta\phi_{l^-,I}$) polar angle between the positive (negative) charge lepton and $\vec{\not{E}}_T$ computed in the Lab frame.
- $\Delta\phi_{\text{CM},I}$: opening angle between the CM system and the I-system.
- $\cos\theta \equiv \hat{\beta}_S^{\text{CM}} \cdot p_{I,T}^S$: the dot product between the direction of the boost from CM to the reconstructed S-frame and the transverse momentum of the I-system in the S-frame.

Finally, jet multiplicities are considered. For the signal samples, the mass associated to the chargino system $M^{\tilde{\chi}^+} = M^{\tilde{\chi}^-}$ will not reproduce the true chargino mass, since the true LSPs are massive and the $I_{a,b}$ systems, in each hemisphere, are simplifications of the neutralino plus neutrino contribution. Nevertheless, the distribution of $M^{\tilde{\chi}^\pm}$ is expected to

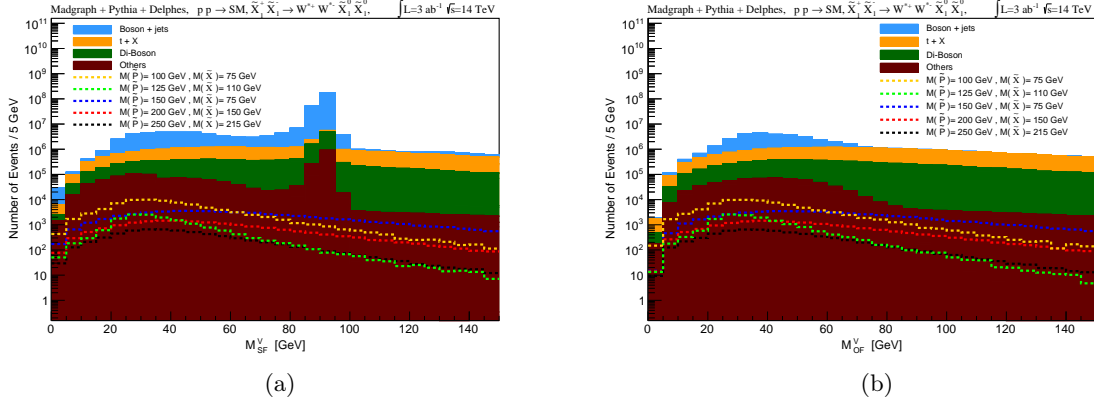


Figure 9: Distribution of the invariant mass of the two leptons for same (a) or different (b) flavor.

be particularly useful to distinguish the signal w.r.t. SM processes with similar kinematics, but where lower mass objects populate one or both the $\tilde{\chi}^\pm$ systems.

The main SM backgrounds are categorized into four groups: 1) Vector boson + jets, mainly populated by $Z \rightarrow \ell^+ \ell^- + \text{jets}$; 2) Production of at least one top quark ($t+X$), with single-top and dileptonic $t\bar{t}$ both contributing; 3) Irreducible di-boson processes mostly arising from W^+W^- with two leptons and missing transverse momentum; and 4) Contributions such as vector boson fusion, tri-boson and gluon fusion plus jets with $h \rightarrow W^+W^-$, are categorized as "others".

Two leptons (electrons and muons) with $p_T > 10$ GeV are required in the final state and at least one jet with $p_T > 20$ GeV, which is associated to the ISR-system. Figure 9 shows the distribution of the invariant mass of the two leptons for same and different flavor, assuming a minimal value for the transverse missing momentum $\cancel{E}_T > 20$ GeV. Standard Model background samples are stacked together, while the overlaid dashed curves refer to chargino pair production samples with different masses and mass splittings. Notice the peak around 90 GeV for same flavor leptons, due to the Standard Model backgrounds containing Z bosons produced in association with jets (in blue), with a moderate contribution from WZ (in green) and vector boson fusion and tri-boson (in red). In the compressed regime the final state events for all the signal distributions tend to populate lower values of M^V and a requirement $M^V < 70$ GeV, or tighter, will be used to specify the signal regions. Notice the additional peak for low values of M^V , arising from $Z + \text{jets}$ and vector boson fusion contributions resulting in a comparable number of events for the cases with two leptons with same or different flavor. The main processes that contribute in this region are $Z \rightarrow \tau^+ \tau^- \rightarrow l^+ l^- \nu \nu \nu \nu$, and moderate contribution from Drell-Yan processes with missing transverse momentum ($Z^*(\gamma^*) \rightarrow \tau^+ \tau^-$) or W boson production, decaying leptonically, with an additional lepton faked by a jet or a photon. For the di-leptonic decay of the Z boson via taus the value for M^V is reconstructed to be below the Z mass, representing a challenge to the analysis in search of compressed charginos.

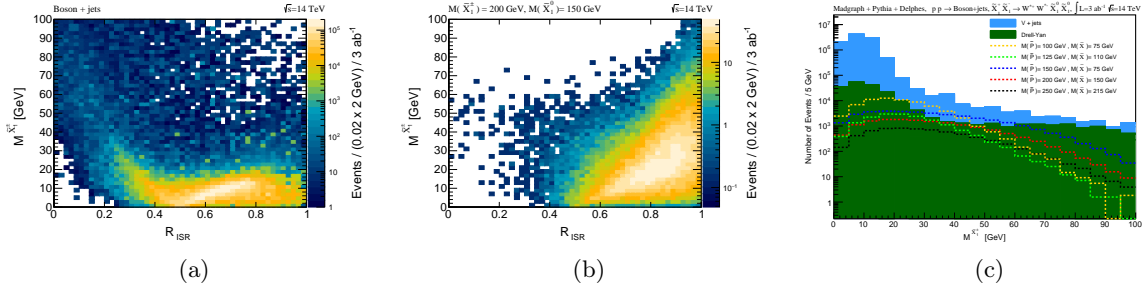


Figure 10: Two-dimensional distribution of $M^{\tilde{\chi}^\pm}$ as a function of R_{ISR} for the Standard Model V +jets background (a) and the signal samples $M_{\tilde{\chi}_1^\pm}=200$ GeV, $M_{\tilde{\chi}_1^0}=150$ GeV (b) and distribution of $M^{\tilde{\chi}^\pm}$ (c) for the events expected per bin for an integrated luminosity of 3 ab^{-1} at $\sqrt{s} = 14$ TeV satisfying the preselection criteria.

Herein, we consider the preselection criteria as follows: final states with two leptons and at least one light jet. A veto is applied for the jets tagged as b , τ and fat: $N_{b\text{-jet}}^{\text{ISR}} = 0$ and $N_{\tau\text{-jet}}^{\text{ISR}} = 0$ and $N_{\text{fat}}^{\text{ISR}} = 0$.¹ A minimal value for the missing transverse momentum ($\cancel{E}_T > 50$ GeV) in concert with $p_{\text{ISR},T}^{\text{CM}} > 50$ GeV is required. In addition, the criterion $M^V < 70$ GeV is imposed. This requirement excludes a large portion of the Standard Model background events, in particular $t\bar{t}$ and multi-bosons processes, independently from the flavor of the two leptons reconstructed. Standard Model processes involving a meson decaying in two same flavor leptons are expected with a small value of the invariant mass $\lesssim 10$ GeV: notably, signal sample events tend to assume larger values.

We present the impact of the main RJR observables sensitive to probe compressed chargino pair mass spectra to reduce the specific Standard Model contribution and progressively, the related selection criteria will be imposed.

Numerous Standard Model processes result in a low value of M^V , in particular the boson plus jets contribution. The focus is on the process $Z \rightarrow \tau^+\tau^- \rightarrow l^+l^-\nu\nu\nu$ plus jets. For such events the role of the chargino system in Figure 8 is assumed by the tau's leptonic decay, while the I systems reconstruct the information of the two neutrinos in each hemisphere. For these background events $M^{\tilde{\chi}^\pm}$ is a reconstruction for the mass of the lepton and two neutrinos resulting from the τ decays. The first two plots in Figure 10 show the two-dimensional distributions between $M^{\tilde{\chi}^\pm}$ and the ratio R_{ISR} for the boson plus jets backgrounds and the signal sample $M_{\tilde{\chi}_1^\pm} = 200$ GeV and $M_{\tilde{\chi}_1^0} = 150$ GeV, Figure 10c shows the distribution of $M^{\tilde{\chi}^\pm}$ for the five signal samples and for the on-shell/off-shell, boson plus jets backgrounds. We demand $M^{\tilde{\chi}^\pm} > 24$ GeV in order to suppress the V +jets background.

With this requirement the SM background is dominated by top processes, specifically a pair of (on- or off-shell) top quarks in the di-leptonic channel. Figure 11 shows the distribution of the light jet multiplicity as a function of the ratio. In order to attenuate the $t\bar{t}$ contribution we demand only one jet in the final state. Despite the $N_{\text{jet}}^{\text{ISR}} = 1$ requirement,

¹In this work a fat jet is defined with $M > 60$ GeV and is a candidate for boosted SM Higgs, vector bosons and top-quark decaying hadronically.

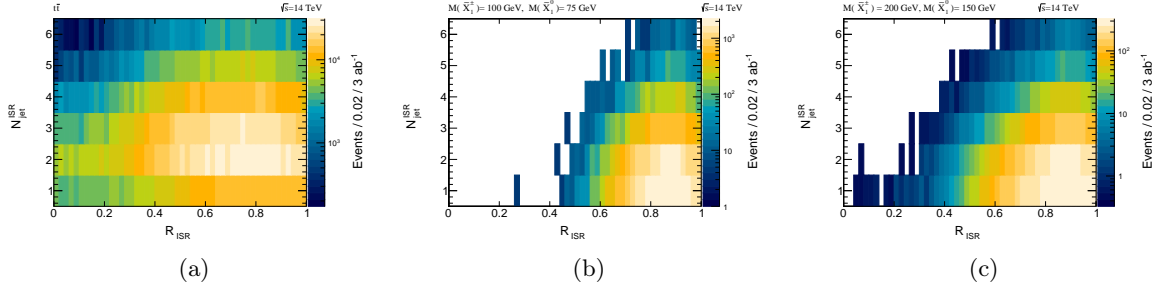


Figure 11: Distribution of $N_{\text{jet}}^{\text{ISR}}$ as a function of R_{ISR} for the Standard Model $t\bar{t}$ background (a) and the signal samples $M_{\tilde{\chi}_1^\pm}=100, 200$ GeV and $M_{\tilde{\chi}_1^0}=75, 150$ GeV in (b and c). We impose preselection criteria and $M_{\tilde{\chi}^\pm} > 24$ GeV.

and vetoing on jets coming from the fragmentation of bottoms, the $t\bar{t}$ background is still not suppressed. If the requirement $N_{\text{fat}}^{\text{ISR}} = 0$ attenuates the contribution with the two jets reconstructed in similar directions, one of the two jets could be outside the geometrical acceptance, mis-measured or of too low momentum to be reconstructed. Also if these events are relatively rare, their contribution is not negligible due to their high cross section $\sigma_{pp \rightarrow t\bar{t}} \sim \mathcal{O}(10^3 \text{ pb})$ at 14 TeV LHC collisions.

Figure 12a shows the distribution of $\Delta\phi_{l+,I}$ for the signal samples and the $t + X$ backgrounds categorized in four sub-processes and stacked together. The events from the top pair contributions tend to populate value close to π , while signal-like events populate low values. Figures 12b and 12c show the two-dimensional distribution $\Delta\phi_{l+,I}$ vs $\Delta\phi_{l-,I}$ for the $t\bar{t}$ background and the signal sample $M_{\tilde{\chi}_1^\pm}=200$ GeV and $M_{\tilde{\chi}_1^0}=150$ GeV, assuming the same selection criteria and requiring $R_{\text{ISR}} > 0.6$. The requirements select background events with kinematics similar to the signal events and in particular we see that a simultaneously large value of $\Delta\phi_{l\pm,I}$ for both the leptons is disfavored. Such events contain predominantly two top quarks produced with low transverse momenta resulting in final states with two reconstructed leptons and one jet not properly tagged. In the transverse plane, one of the two leptons is expected to fly close to the reconstructed jet (associated to the ISR-system), while the other is expected to be closer to the invisible system. As a consequence background events tend to assume larger values of $\Delta\phi_{l+,I} + \Delta\phi_{l-,I}$ than signal events. A similar two-dimensional distribution as in Figure 12c is demonstrated by all signal samples studied. To attenuate the $t+X$ background one requires a unique light jet associated to the ISR-system and in addition $\Delta\phi_{l+,I} + \Delta\phi_{l-,I} < 2$.

Applying these selection criteria, the dominant Standard Model contribution is the irreducible di-boson background: W^+W^- . The goal is to distinguish between signal and background events with similar event topologies and kinematics, in particular when selection criteria close to the final configuration are applied. The key difference to exploit is that of the I-system ($I_a + I_b$) for the W^+W^- background composed of two neutrinos, while the signal events have four weakly interacting particles comprising the invisible system.

Figure 13 shows the main angular observables sensitive to separate events resulting from

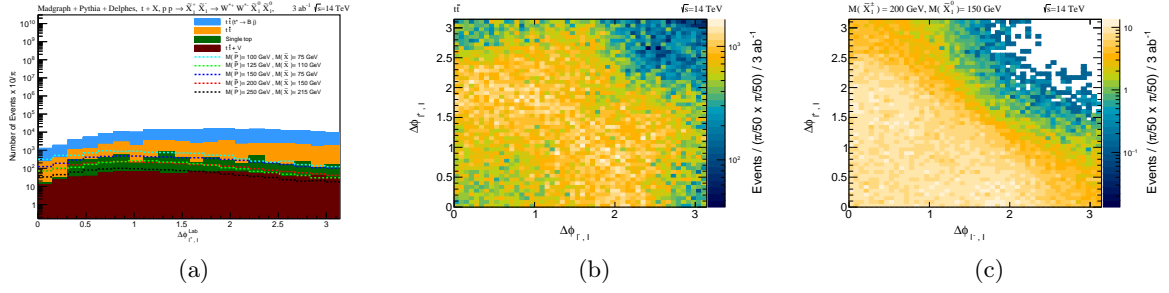


Figure 12: Distribution of $\Delta\phi_{l+,l}$ for Standard Model $t + X$ background and signal events passing preselection criteria and the additional requirements $M_{\tilde{\chi}^\pm} > 24$ GeV and $N_{\text{jet}}^{\text{ISR}} = 1$ (a). Two-dimensional distribution of the opening angles between the leptons and the I-system for the $t\bar{t}$ background (b) and the signal sample $M_{\tilde{\chi}_1^\pm} = 200$ GeV, $M_{\tilde{\chi}_1^0} = 150$ GeV (c) imposing $R_{\text{ISR}} > 0.6$.

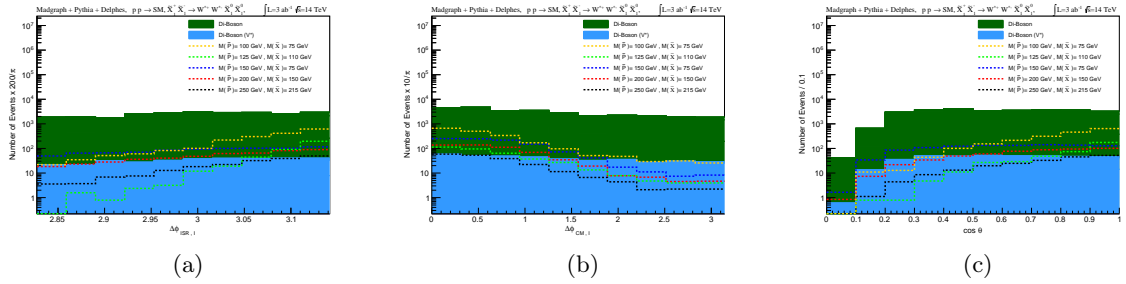


Figure 13: Distributions of angular RJR observables for signal samples and di-boson Standard Model background, for events passing preselection criteria and the additional requirements $M_{\tilde{\chi}^\pm} > 24$ GeV, $N_{\text{jet}}^{\text{ISR}} = 1$, $R_{\text{ISR}} > 0.6$ and $\Delta\phi_{l+,l} + \Delta\phi_{l-,l} < 2$.

compressed chargino samples with respect to WW decays. Figure 13a shows the distribution of $\Delta\phi_{\text{ISR},l}$. Signal events tend to populate values closer to π , as the mass difference $\Delta M = M_{\tilde{P}} - M_{\tilde{\chi}}$ is reduced. Figure 13b shows the distribution of the angle between the CM and I-system, where in this case signal events towards zero, almost independently of ΔM or $M_{\tilde{P}}/M_{\tilde{\chi}}$. The distribution of $\cos\theta \equiv \hat{p}_{\tilde{S}}^{\text{CM}} \cdot p_{l,T}^{\text{S}}$ is shown in Figure 13c.

Selection criteria defined with the compressed RJR observables result in signal regions used to investigate chargino pair production in final states with two leptons and missing transverse momentum. The requirements for the observable R_{ISR} are tuned depending on the mass ratio and are more stringent than the chargino-neutralino associated study due to the larger multiplicity of weakly interacting particles in the final state.

Figure 14 shows the distributions of R_{ISR} and $M_{\tilde{\chi}^\pm}$ for SM background and signal sample events passing the selection criteria in Table 2. For the lowest mass splitting the requirement $R_{\text{ISR}} > 0.85$ is applied only for the sample $M_{\tilde{\chi}_1^\pm} = 100$ GeV, while for $\Delta M = 25$ GeV one demands this criterion for three samples ($M_{\tilde{\chi}_1^\pm} \leq 150$ GeV).

The signal regions expressed by the selection criteria of the RJR observables defined in

	Mass Splitting [GeV]				
Variable	$\Delta M = 15$	$\Delta M = 25$	$\Delta M = 35$	$\Delta M = 50$	$\Delta M = 75$
Object multiplicity selection criteria	2 OS Leptons (e and μ) with $p_T^{lep} > 10$ GeV, $N_{jet}^{\text{ISR}} = 1$, $N_{b\text{-jet}}^{\text{ISR}} = 0$, $N_{\tau\text{-jet}}^{\text{ISR}} = 0$ and $N_{\text{fat}}^{\text{ISR}} = 0$				
$p_{\text{ISR},T}^{\text{CM}}(\cancel{E}_T) > [\text{GeV}]$	50				
$M^{\text{V}} < [\text{GeV}]$	50			60	70
$\Delta\phi_{\text{I}^+, \text{I}} + \Delta\phi_{\text{I}^-, \text{I}} <$	2				
$M^{\tilde{\chi}_1^\pm} > [\text{GeV}]$	24				
$\Delta\phi_{\text{CM}, \text{I}} <$	0.5	0.5	0.45		
$\Delta\phi_{\text{ISR}, \text{I}} >$	3.12	3.10	3.06	3.05	3.04
$\cos\theta >$	0.9	0.85	0.8	0.75	0.7
$R_{\text{ISR}} >$	0.85, 0.9	0.85, 0.9	0.8, 0.85 0.9	0.8, 0.85	0.75, 0.8 0.85

Table 2: Selection criteria for signal regions in the analysis of chargino pair production in final states with two leptons and missing transverse energy.

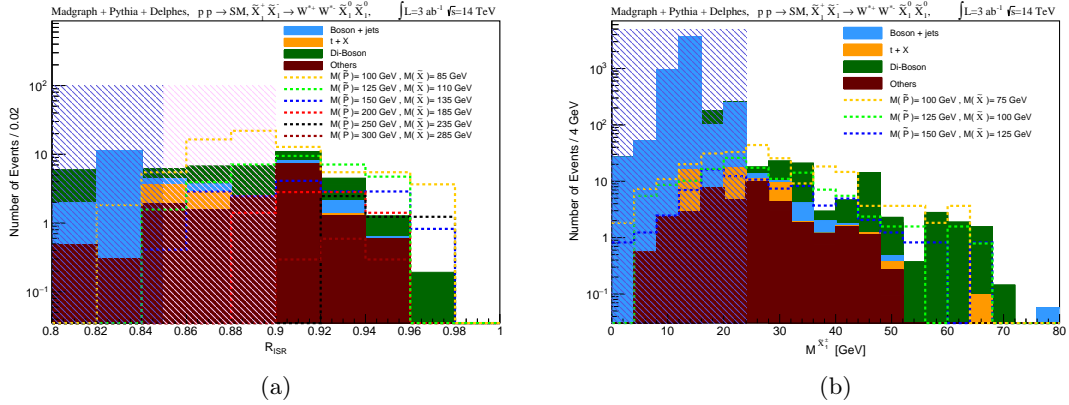


Figure 14: The distributions of R_{ISR} for the signal and BG events passing the N-1 selection criteria in Table 2 column 1 (a) and of $M_{\tilde{\chi}_1^\pm}$ imposing the requirements in column 2 with $R_{ISR} > 0.85$ (b).

Table 2 are applied to calculate projected sensitivities for compressed spectra signal samples. Figure 15 shows the value of Z_{Bi} , the binomial score representing the significance of a given signal expressed in standard deviations in the presence of a background hypothesis, at $\sqrt{s}=14$ TeV for an integrated luminosity of 3000 fb^{-1} . One considers a systematic uncertainty of 20% for the overall Standard Model background: a compromise between a large data sample projection (10 times the integrated luminosity of the associated chargino-neutralino production analysis) and stringent selection criteria assumed to suppress the background yields.

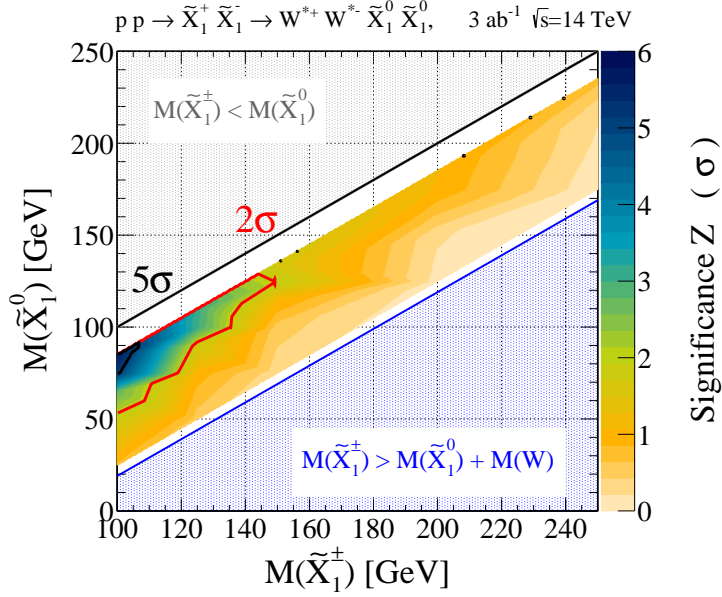


Figure 15: Projected Z-value for chargino pair production in the compressed region ($15 \text{ GeV} \leq \Delta M \leq 75 \text{ GeV}$) at $\sqrt{s} = 14 \text{ TeV}$ assuming a systematic uncertainty of 20% for the SM background for an integrated luminosity of 3000 fb^{-1} .

Exploiting the RJR technique and with enough data collection one can set limits for the compressed chargino pair production topology at LHC14, with masses $\sim 150 \text{ GeV}$ being excluded in the best scenarios.

4 Conclusions

We have introduced an original approach to searches for compressed electroweakinos based on the imposition of the decay trees as in Figures 1 and 8 for the interpretation of reconstructed events, using the Recursive Jigsaw Reconstruction technique.

Putative wino-like chargino neutralinos could be discovered at LHC14 with masses $M_{\tilde{\chi}_1^\pm} = M_{\tilde{\chi}_2^0} > 150 \text{ GeV}$ for a large portion of the samples investigated ($15 \text{ GeV} \lesssim \Delta M \lesssim 50 \text{ GeV}$) assuming an integrated luminosity of 300 fb^{-1} and leveraging on only *transverse* observables. The RJR technique is sensitive to the extremely challenging chargino pair topology scenarios in the compressed regime. A strategy based on several experimental observables has been used to reduce the W^+W^- and the other main background yields due to the necessity of requiring jets in the final state to be associated to the ISR-system. A potential 95% confidence level exclusion limit can be obtained for an assumed data set of 3 ab^{-1} assuming a 20% of systematic uncertainty for sample spectra with $\Delta M \lesssim 50 \text{ GeV}$.

For both the topologies, the signal yields in the extreme compressed scenarios can benefit from an improvement in the efficiencies of the detector in the reconstruction of low transverse momentum leptons ($< 10 \text{ GeV}$). On the other hand, for large mass splittings ($\Delta M \gtrsim M_Z$) the bulk analysis should be preferred to a compressed investigation, while for intermediate scenarios $50 \text{ GeV} \lesssim \Delta M \lesssim M_Z$ one can exploit the complementarity of

observables based on a reconstruction of the event with or without the ISR-system and include cases with vector bosons decaying hadronically.

The method is expected to have still more impact in the cases of final state topologies with larger lepton multiplicity: pair production of charginos and/or neutralinos with slepton mediated decays. The RJR technique can be extended to these studies and to the pair production of heavy neutralinos in final states with four leptons exploiting the simplified tree in Figure 1, with a simple modification in the assignment of the objects in the case of sleptons of the third generation.

The results from the simplified models investigated in this work can be partially reinterpreted assuming different compositions for the electroweakinos. The method can be applied for higgsino-dominated charginos and neutralinos, with the latter decaying via an off-shell Standard Model Higgs boson, requiring two b -jets and one lepton in the V-system. For chargino pair production with a mixed higgsino-wino nature, one can re-weight the signal yields with the appropriate cross sections: typically the contributions from off-shell charged Higgs or other particles can be neglected since $M_S, M_{H^\pm} \gg M_W$ in most SUSY models.

References

- [1] H. Miyazawa, *Baryon Number Changing Currents*, *Prog. Theor. Phys.* **36** (1966) 1266–1276.
- [2] P. Ramond, *Dual Theory for Free Fermions*, *Phys. Rev.* **D3** (1971) 2415–2418.
- [3] Y. Golfand and E. Likhtman, *Extension of the Algebra of Poincare Group Generators and Violation of p Invariance*, *JETP Lett.* **13** (1971) 323–326.
- [4] A. Neveu and J. Schwarz, *Factorizable dual model of pions*, *Nucl. Phys.* **B31** (1971) 86–112.
- [5] A. Neveu and J. Schwarz, *Quark Model of Dual Pions*, *Phys. Rev.* **D4** (1971) 1109–1111.
- [6] D. Volkov and V. Akulov, *Is the Neutrino a Goldstone Particle?*, *Phys. Lett.* **B46** (1973) 109–110.
- [7] J. Wess and B. Zumino, *A lagrangian model invariant under supergauge transformations*, *Phys. Lett.* **B49** (1974) 52 – 54.
- [8] J. Wess and B. Zumino, *Supergauge Transformations in Four-Dimensions*, *Nucl. Phys.* **B70** (1974) 39–50.
- [9] H. An and L.-T. Wang, *Opening up the compressed region of top squark searches at 13 TeV LHC*, *Phys. Rev. Lett.* **115** (2015) 181602, [[arxiv:1506.00653](#)].
- [10] I. Hinchliffe, F. E. Paige, M. D. Shapiro, J. Soderqvist and W. Yao, *Precision SUSY measurements at CERN LHC*, *Phys. Rev.* **D55** (1997) 5520–5540, [[arxiv:9610.544](#)].
- [11] ATLAS collaboration, *Search for squarks and gluinos in final states with jets and missing transverse momentum using 36 1/fb of $\sqrt{s} = 13$ TeV pp collision data with the ATLAS detector*, *Tech. Rep.* ATLAS-CONF-2017-022.
- [12] R. Barbieri and G. F. Giudice, *Upper Bounds on Supersymmetric Particle Masses*, *Nucl. Phys.* **B306** (1988) 63–76.
- [13] C. Rogan and P. Jackson, *Recursive Jigsaw Reconstruction: HEP event analysis in the presence of kinematic and combinatoric ambiguities*, [arxiv:1705.10733](#).

- [14] P. Jackson, C. Rogan and M. Santoni, *Sparticles in motion: Analyzing compressed susy scenarios with a new method of event reconstruction*, *Phys. Rev.* **D95** (2017) 035031 [[arxiv:1607.08307](#)].
- [15] J. Anderson, A. Avetisyan, R. Brock, S. Chekanov, T. Cohen et al., *Snowmass Energy Frontier Simulations*, [arxiv:1309.1057](#).
- [16] J. Alwall, M. Herquet, F. Maltoni, O. Mattelaer and T. Stelzer, *MadGraph 5 : Going Beyond*, *JHEP* **1106** (2011) 128, [[arxiv:1106.0522](#)].
- [17] T. Sjostrand, S. Mrenna and P. Z. Skands, *PYTHIA 6.4 Physics and Manual*, *JHEP* **05** (2006) 026, [[arxiv:0603.175](#)].
- [18] M. Selvaggi, *DELPHES 3: A modular framework for fast-simulation of generic collider experiments*, *J.Phys.Conf.Ser.* **523** (2014) 012033.
- [19] M. Cacciari, G. P. Salam, G. Soyez, *The Anti- $k(t)$ jet clustering algorithm*, *JHEP* **0804** (2008) 063, [[arxiv:0802.1189](#)].
- [20] M. Cacciari, G. P. Salam, G. Soyez, *FastJet user manual*, *Eur. Phys. J. C* **72** (2012) 1896.
- [21] ATLAS COLLABORATION, G. Aad et al., *The ATLAS Experiment at the CERN Large Hadron Collider*, *JINST* **3** (2008) S08003.
- [22] CMS COLLABORATION, S. Chatrchyan et al., *The CMS experiment at the CERN LHC*, *JINST* **3** (2008) S08004.
- [23] A. Avetisyan, J. M. Campbell, T. Cohen, N. Dhingra, J. Hirschauer et al., *Methods and Results for Standard Model Event Generation at $\sqrt{s} = 14$ TeV, 33 TeV and 100 TeV Proton Colliders (A Snowmass Whitepaper)*, [arxiv:1308.1636](#).
- [24] B. Fuks, M. Klasen, D. R. Lamprea and M. Rothering, *Gaugino production in proton-proton collisions at a center-of-mass energy of 8 TeV*, *JHEP* **10** (2012) 081, [[arxiv:1207.2159](#)].
- [25] B. Fuks, M. Klasen, D. R. Lamprea and M. Rothering, *Precision predictions for electroweak superpartner production at hadron colliders with RESUMMINO*, *Eur. Phys. J. C* **73** (2013) 2480, [[arxiv:1304.0790](#)].
- [26] CMS COLLABORATION, *Search for new physics in the compressed mass spectra scenario using events with two soft opposite-sign leptons and missing momentum energy at 13 TeV*, [CMS-PAS-SUS-16-025](#).
- [27] R. D. Cousins, J. T. Linnemann and J. Tucker, *Evaluation of three methods for calculating statistical significance when incorporating a systematic uncertainty into a test of the background-only hypothesis for a Poisson process*, *Nucl. Instrum. Meth.* **A595** (2008) 480–501.
- [28] ATLAS COLLABORATION, *Search for direct production of charginos, neutralinos and sleptons in final states with two leptons and missing transverse momentum in pp collisions at $\sqrt{s} = 8$ TeV with the ATLAS detector*, *JHEP* **05** (2014) 071, [[arxiv:1403.5294](#)].
- [29] P. Jackson, *The Recursive Jigsaw Reconstruction Technique*, *PoS ICHEP2016* (2017) 1219
- [30] P. Jackson, *Compressed SUSY searches with Recursive Jigsaw Reconstruction*, *PoS EPS-HEP2017* (2017) 292